JES Bulletin, 3(1):08-12, Jan – 2025

Open Access, Peer Reviewed, Research Journal
©JES Printer and Publisher
Print & Online available on https://jesbulletin.in

Research Article

Synthesis of $Cu_{1-x}Bi_xFe_2O_4$ nanoparticles via sol-gel auto-combustion method and their structural properties

Devendra Dadarao Narwade[a], *Vivekanand B. Kawade*[b]

[a]*Department of Physics, Deogiri College, Chhatrapti Sambhajinagar 431001 INDIA*
[b]*Department of Physics, L.L.D. Mahila Mahavidyalay,Parli Vaijnath, Dist. Beed 431515 INDIA*

Corresponding Author:

ARTICLE INFO

Received: 10/02/2024
Revised: 15/03/2024
Accepted: 01/04/2024

KEYWORDS

Nanoparticles, Sol-gel, Bismuth ferrite, *XRD*, Williamson Hall method

ABSTRACT

Copper ferrite ($CuFe_2O_4$) nanoparticles have made significant interest due to their multifunctional properties, including magnetic, catalytic, and electronic applications. Doping copper ferrite with bismuth (Bi^{3+}) can further tailor these properties for specific applications. This study reports the sol-gel synthesis and characterization of bismuth-doped copper ferrite ($Cu_{1-x}Bi_xFe_2O_4$) nanoparticles. The structural; morphological; magnetic, and optical properties of the synthesized nanoparticles were analyzed using X-ray diffraction (XRD), Willianmson-Hall Extrapolation. Results demonstrate the successful incorporation of (Bi^{3+}) into the spinel structure and reveal the impact of (Bi^{3+}) substitution on structural properties. These findings highlight the potential of $Cu_{1-x}Bi_xFe_2O_4$ nanoparticles in advanced material applications.

1 Introduction

Copper ferrite ($CuFe_2O_4$) is a well-known spinel ferrite material that has attracted considerable attention due to its diverse applications across fields such as magnetics, catalysis, and energy storage. The intrinsic multifunctional properties arise from its spinel structure, which enables flexibility in ionic distribution between tetrahedral (A) and Octahedral (B) sites. This characteristic makes $CuFe_2O_4$ a versatile material for the advanced technologies, including spintronics, photocatalysis, electromagnetic interference (EMI) shielding [1], and energy storage devices [2]. Despite its promising properties, there is a growing demand to further optimize the structural behavior of $CuFe_2O_4$ to meet the specific requirements of emerging technologies. One of the most effective strategies for tailoring the properties of ferrites is doping, wherein substituting metal ions within the spinel lattice induces significant changes in cation distribution, lattice strain, and electronic structure. Among various dopants explored, bismuth (Bi^{3+}) stands out as a promising candidate due to its unique electronic configuration, large ionic radius, and multivalent nature. (Bi^{3+}) doping has the potential to alter the magnetic interactions, electron hopping mechanisms, and crystal field effects within the ferrite matrix, enabling precise control over its functional properties. These modifications are especially relevant for applications in areas such as optoelectronics, photocatalysis, and environmental remediation. The synthesis method plays a major and critical role in determining the structural and functional properties of $Cu_{1-x}Bi_xFe_2O_4$ nanoparticles (See **Figure 1**). The sol-gel method is widely regarded as a versatile, cost-effective, and scalable approach for synthesizing nanoparticles with high purity, controlled stoichiometry, and uniform morphology [3]. This method also offers fine control over particle size and crystallinity, making it particularly suitable for producing doped ferrite materials. In this study, bismuth-doped copper ferrite ($Cu_{1-x}Bi_xFe_2O_4$) nanoparticles were synthesized using the sol-gel technique, and the effects of Bi^{3+} substitution on their structural properties were systematically investigated. The characterization was performed using techniques such as X-ray diffraction (XRD), Williamson-Hall Function ($W-H\ Plot$). This study aims to provide a deeper understanding of the role of Bi doping in modifying the structural and functional properties of $CuFe_2O_4$. By systematically exploring the effects of Bi substitution, this research paper not only contributes to enhance body of knowledge on the doped ferrites but also positions $Cu_{1-x}Bi_xFe_2O_4$ nanoparticles as promising materials for advanced technological applications. The findings open new avenues for the design and optimization of multifunctional ferrite

materials through doping strategies and highlight the potential for real-world applications in magnetic data storage, catalysis, and environmental remediation.

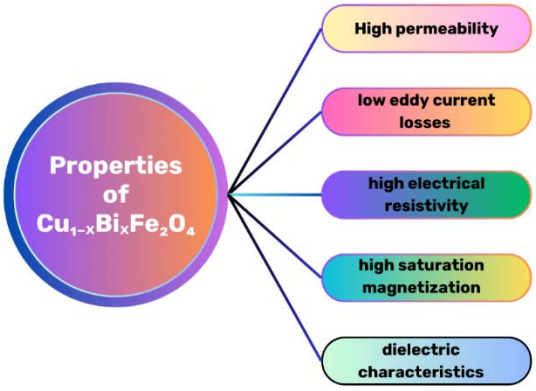

Figure 1. *Properties of $Cu_{1-x}Bi_xFe_2O_4$ nanoparticles*

Structure of $Cu_{1-x}Bi_xFe_2O_4$ nanoparticles

$Cu_{1-x}Bi_xFe_2O_4$ nanoparticles possess a spinel ferrite crystal structural properties, identified as a cubic close-packed oxygen lattice with cations occupying tetrahedral (A) and octahedral (B) sites. In undoped $CuFe_2O_4$, an inverse spinel structure prevails, where Fe^{3+} ions (0.645 Å) [4] occupy both (A) and $[B]$ sites, while Cu^{2+} ions (0.73 Å) [5] primarily reside on $[B]$ sites. The standard lattice parameter for undoped $CuFe_2O_4$ is approximately 8.38 Å, though it can vary slightly depending on synthesis conditions. The incorporation of larger Bi^{3+} ions (1.03 Å) [6] into the lattice preferentially replaces Cu^{2+} ions at the $[B]$ sites. This substitution leads to lattice expansion, evident from X-ray diffraction data, and induces strain within the spinel structure. To maintain charge neutrality and structural stability, the distribution of Fe^{3+} ions between A and B sites is also influenced by Bi^{3+} incorporation. Furthermore, the substitution of Cu^{2+} by Bi^{3+} introduces charge imbalance, which is often compensated by the formation of oxygen (1.40 Å) or cationic vacancies. From an atomic perspective, the spinel lattice contains 8 formula units per unit cell, with 32 oxygen ions forming a face-centered cubic array FCC space group; Fd3m. The atomic weights of $Cu, Fe,$ and O are $63.55\ u$, $55.85\ u$, and $16.00\ u$, respectively [7]. Doping with Bi^{3+} $(208.98\ u)$ significantly increases the molecular weight of the compound. At low doping levels (x), the spinel structure remains relatively intact with minor lattice distortions. However, higher doping concentrations can lead to substantial structural changes, including significant lattice expansion and potential phase segregation. These structural modifications directly impact the material's functional properties, such as magnetic behavior, optical bandgap, and electrical conductivity. Consequently, $Cu_{1-x}Bi_xFe_2O_4$ nanoparticles exhibit tunable crystal structures and properties, making them promising candidates for advanced applications in magnetics, optoelectronics, and catalysis.

2 2. Experimental

2.1 2.1 Materials

High-purity analytical reagents (AR-grade) sourced from Fisher Scientific Pvt Ltd were employed for the synthesis process, ensuring precision and reliable experimental outcomes. These reagents, with a purity level of 99.9%, were specifically chosen to meet the demanding standards of advanced laboratory instrumentation. The precursors used in this study included copper nitrate trihydrate $(Cu(NO_3)_2 \cdot 3H_2O)$; bismuth nitrate pentahydrate $(Bi(NO_3)_3 \cdot 5H_2O)$; ferric nitrate nonahydrate $(Fe(NO_3)_3 \cdot 9H_2O)$; in combination with citric acid $(C_6H_8O_7)$, and ammonia solution (NH_3). Citric acid served as a chelating agent, facilitating uniform mixing of the metal ions, while ammonia solution controlled the pH, enabling efficient precipitation. Deionized water, used as the solvent, minimized the risk of impurity interference. Given the high purity of the chemicals, further purification steps were deemed unnecessary. This meticulous selection and utilization of reagents were crucial for maintaining the integrity of the synthesis process and ensuring the reproducibility and accuracy of the research findings, thereby upholding the rigorous standards of scientific inquiry.

2.2 2.2 Synthesis of $Cu_{1-x}Bi_xFe_2O_4$ nanoparticles

The $Cu_{1-x}Bi_xFe_2O_4$ nanoparticles were fabricated using the sol-gel method, following a series of carefully controlled steps to ensure uniformity and high purity of the final product. First, accurately weighed amounts of copper nitrate trihydrate $(Cu(NO_3)_2 \cdot 3H_2O)$, bismuth nitrate pentahydrate $(Bi(NO_3)_3 \cdot 5H_2O)$, and ferric nitrate nonahydrate $(Fe(NO_3)_3 \cdot 9H_2O)$ were dissolved in distilled water under constant stirring to form a homogeneous aqueous solution. The molar ratios of these precursors were adjusted based on the desired stoichiometry of $Cu_{1-x}Bi_xFe_2O_4$, with the doping level x ranging from $0\ to\ 1$. To facilitate the complexation of metal ions, citric acid $(C_6H_8O_7)$ was added in a 1:3 molar ratio with the total metal ions, preventing premature precipitation and ensuring the uniform and clear distribution of the ions in the solution. The mixture was stirred continuously until a clear, homogeneous solution was obtained. Next, the pH of the solution was adjusted to 7 by slowly adding ammonia solution (NH_3) dropwise while monitoring with a pH meter. This pH adjustment helped promote the formation of a stable sol, with continuous stirring preventing localized precipitation and maintaining solution uniformity. The sol was then gradually heated on a hot plate at a temperature of $80-90°C$. As the water and volatile components evaporated, a viscous gel began to form. The heating process was carefully controlled to ensure uniform gelation.The viscous gel was transferred to the oven to dry and kept at $100°C$ for 12 hours to remove residual water and volatile organic compounds, resulting in a xerogel, a porous and brittle intermediate solid. For the crystallization of the spinel ferrite phase, the xerogel was subjected to calcination in a muffle furnace at temperatures between $500°C$ and $600°C$ for 4 hours in air. The heating rate during calcination was controlled at $5°C/min$ to avoid thermal shocks and ensure the

development of a well-ordered crystalline structure. After calcination, the resulting $Cu_{1-x}Bi_xFe_2O_4$ nanoparticles were allowed to cool to room temperature, then collected and stored for further characterization.

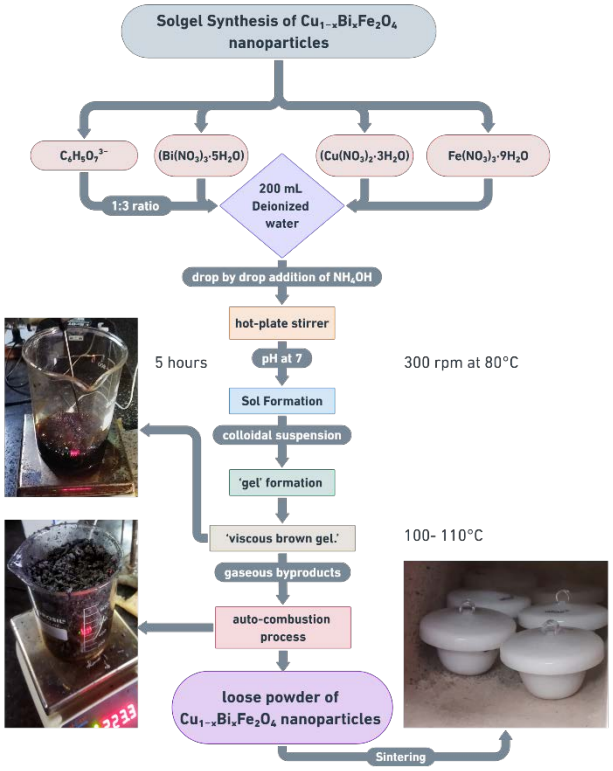

Figure 1 schematic overview of sol-gel auto-combustion synthesis process of $Cu_{1-x}Bi_xFe_2O_4$ nanoparticles

2.3 Characterizations techniques

The $Cu_{1-x}Bi_xFe_2O_4$ nanoparticles were characterized using several techniques to investigate their structural, morphological, magnetic, and optical properties. X-ray Diffraction (XRD) was employed to analyze the consisting phase composition of the material and crystallite size of the nanoparticles, using a Bruker $D-8$ X-ray diffractometer. The instrument operated under precise conditions with a voltage of 45 kV and a current of $30\,mA$, collecting diffraction patterns in the 2θ range of 10° to 80° using Cu Kα radiation ($\lambda = 1.5406$ Å) at a scanning speed of $0.02\,°/s$. The data obtained provided insights into the crystallinity and particle size of the synthesized material. Williamson-Hall extrapolation function was plot to veryfy the results obtained from XRD data.

3 Results and discussion

3.1 X-ray diffraction of $Cu_{1-x}Bi_xFe_2O_4$ nanoparticles

Figure 2 presents the X-ray diffraction (XRD) pattern of $Cu_{1-x}Bi_xFe_2O_4$ nanoparticles synthesized via the sol-gel auto-combustion method at room temperature, covering a (2θ) range of 20°– 80°.

Table 1. Miller Indices of the $Cu_{1-x}Bi_xFe_2O_4$ nanoparticles

2θ (degrees)	hkl Plane	Remarks
~18.3	111	Weak peak, indicates spinel phase
~30.3	220	First major peak of spinel structure
~35.7	311	Characteristic strong peak for spinels
~43.3	400	Secondary intense peak
~53.8	422	Moderate intensity
~57.3	511	High symmetry plane
~62.9	440	Strong peak, confirms spinel formation

Figure 2 X-ray diffraction (XRD) pattern of $Cu_{1-x}Bi_xFe_2O_4$ nanoparticles

The diffraction pattern confirms the formation of a spinel structure with (hkl) planes, corresponding to the $Fd3m - Oh7$ space group [8]. The XRD pattern of $Cu_{1-x}Bi_xFe_2O_4$ nanoparticles exhibits diffraction peaks characteristic of a cubic spinel ferrite structure. The prominent peaks observed at approximately 2θ values of 18.3°, 30.3°, 35.7°, 43.3°, 53.8°, 57.3°, and 62.9° correspond to the hkl planes $(111), (220), (311), (400), (422), (511)$, and (440), respectively [9]. These planes are indicative of the spinel phase typically associated with $CuFe_2O_4$. The intense peak at ~35.7° corresponding to the (311) plane is a hallmark of spinel ferrites and confirms the successful formation of the desired crystalline phase. The substitution of Cu^{2+} ions with Bi^{3+} ions does not disrupt the spinel structure but may cause slight peak shifts due to lattice distortion, reflecting the larger ionic radius of Bi^{3+}. Such distortions can alter the lattice parameter, which can be calculated using the d-spacing and hkl indices. Additionally, the crystallite size can be determined using the Scherrer equation, with the (311) peak typically chosen for accurate size estimation. The results collectively confirm the spinel structure of the synthesized nanoparticles and the effective incorporation of bismuth into the $CuFe_2O_4$ matrix [10]. $Cu_{1-x}Bi_xFe_2O_4$ nanoparticles possese an inverse cubic spinel structure; where Co^{2+} ions occupy the octahedral $[B]$ sites, and Fe^{3+} ions are distributed across both the tetrahedral (A) and octahedral $[B]$ sites [11]. Importantly, no impurity peaks were observed in the diffraction pattern, indicating the purity of the synthesized sample. Structural properties are listed in Table 1, with the lattice parameter calculated using the appropriate formula. [12],

$$a = d_{hkl}\sqrt{h^2 + k^2 + l^2} \quad (1)$$

Where (d) represents the interplanar distance of two planes, (a) represents the lattice constant, and (hkl) represents the miller indices of each plane in the XRD plane family. The lattice parameter value of $Cu_{1-x}Bi_xFe_2O_4$ nanoparticles was determined by Debye-formula. Scherrer's [13],

$$D = \frac{k\lambda}{\beta \cos\theta} \quad (2)$$

Here, k is the constant with the value of 0.89, is the wavelength of the X-ray light source (1.54051 Å); β is the full width at half maximum $(FWHM)$, and is the glancing angle. The average lattice constant was found to be approximately ~8.385 Å, confirming the formation of a well-structured cubic spinel crystal with minimal distortions. These results indicate that the nanoparticles were synthesized with high crystalline quality, consistent with the expected characteristics of ferrite materials. The decrease in d-spacing with increasing Bragg's angle aligns with standard crystallographic behavior, confirming the accuracy of the measurements and the integrity of the synthesized material. Using the relationship, the X-ray density (dX) of $Cu_{1-x}Bi_xFe_2O_4$ nanoparticles (5.439 $gm/cm3$) was calculated [14],

$$d_x = {}^{8M}/_{N_A a^3} \quad (3)$$

Where dx is the X-ray density and M is the composition's relative molecular weight. The multiplication factor 8 was utilised as there are 8 formula units in to unit cell. N_A is the Avogadro's number

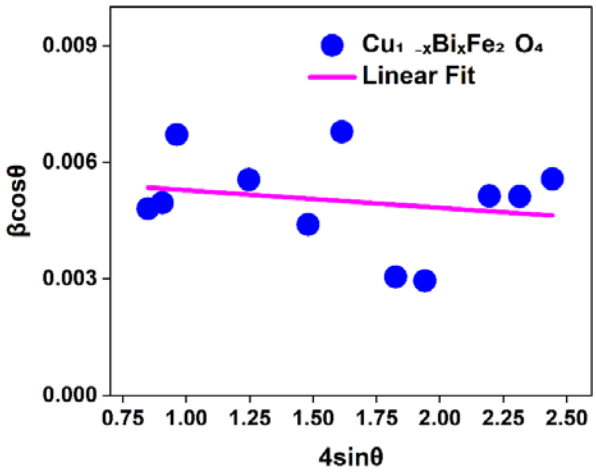

Figure 3 Williamson-Hall Plot of $Cu_{1-x}Bi_xFe_2O_4$ nanoparticles

The corrected FWHM data is then used to plot the Williamson-Hall equation, which indicates the broadening of X-ray diffraction peaks to both crystallite size (t) and microstrain $\beta_T = \beta_D + \beta_\varepsilon$. The equation is $\beta_T\, cos\theta = \varepsilon(4sin\theta) + \frac{k\lambda}{D}$, where β is the corrected broadening, θ\thetaθ is the diffraction angle, λ is the X-ray wavelength, L is the crystallite size, and ϵ\epsilonϵ is the microstrain [15]. The plot of $\beta \cdot cos\theta$ versus $4sin\theta$ should yield a straight line, where the slope corresponds to the microstrain and the intercept provides the crystallite size. The crystallite size L and the microstrain ε are then extracted from the slope and intercept, respectively, allowing for the characterization of the $Cu_{1-x}Bi_xFe_2O_4$ nanoparticles. This method provides valuable insights into the structural properties of the material, which are important for understanding its performance in various applications. [16].

4 Conclusions

The sol-gel synthesis and characterization of bismuth-doped copper ferrite ($Cu_{1-x}Bi_xFe_2O_4$) nanoparticles have demonstrated the successful incorporation of Bi^{3+} into the spinel structure, leading to significant alteration in the structural, magnetic, and optical properties of the material. The results obtained has highlighted the potential of Bi doping as an effective strategy to tailor the properties of $CuFe_2O_4$ for perticular applications, enhancing its performance in areas such as magnetics, catalysis, energy storage adaptiveness, and environmental applications. The Williamson-Hall analysis further supports the understanding of how Bi substitution impacts the crystallite size and microstrain, that contributing to the overall material's behavior. These findings not only provide valuable insights into the effects of doping on $CuFe_2O_4$ but also position $Cu_{1-x}Bi_xFe_2O_4$ nanoparticles as promising candidates for advanced technological applications. The successful synthesis of high-quality doped ferrites via the sol-gel method opens up new opportunities for the design and optimization of multifunctional materials, offering exciting possibilities for innovation in emerging fields such as optoelectronics, photocatalysis, and magnetic data storage.

Reference

[1] S. Iqbal, H. Khatoon, R. Kotnala, S. Ahmad, Bi-doped barium ferrite decorated polythiophene nanocomposite: influence of Bi-doping on structure, morphology, thermal and EMI shielding behavior for X-band, Journal of Materials Science, 55 (2020) 15894-15907.

[2] A. Ramadan, W. Ramadan, Superior performance of asymmetric supercapacitor based on Cu doped bismuth ferrite electrode, Journal of Energy Storage, 100 (2024) 113702.

[3] W.A. Wani, S. Kundu, K. Ramaswamy, H. Venkataraman, Structural, morphological, optical and dielectric investigations in cobalt doped bismuth ferrite nanoceramics prepared using the sol-gel citrate precursor method, Journal of Alloys and Compounds, 846 (2020) 156334.

[4] K. Manjunatha, T.-E. Hsu, H.-H. Chiu, M.-K. Ho, B. Chethan, M.C. Oliveira, E. Longo, R.A. Ribeiro, S.-L. Yu, C.-L. Cheng, Bismuth-doping induced enhanced humidity sensing properties of spinel NiFe2O4 nanoparticles, Sensors and Actuators B: Chemical, 422 (2025) 136645.

[5] R. Norrestam, The effective shapes and sizes of Cu2+ and Mn3+ ions in oxides and fluorides, Zeitschrift für Kristallographie-Crystalline Materials, 209 (1994) 99-106.

[6] J. Xu, Y. Pan, T. Tian, C. Mao, H. Feng, Y. Ma, H. Shao, Effective enhancement of light yield achieved in Bi4Si3O12 scintillation single crystals by doping with tantalum ions, Journal of Alloys and Compounds, 960 (2023) 170754.

[7] M.E. Wieser, T.B. Coplen, Atomic weights of the elements 2009 (IUPAC Technical Report), Pure and Applied Chemistry, 83 (2010) 359-396.

[8] Z. Zi, S. Zhang, B. Wang, X. Zhu, Z. Yang, J. Dai, W. Song, Y. Sun, Morphology and magnetic properties of Co0. 8Fe2. 2O4 films prepared by the chemical solution deposition, Journal of magnetism and magnetic materials, 322 (2010) 148-151.

[9] K.L. Routray, D. Sanyal, D. Behera, Dielectric, magnetic, ferroelectric, and Mossbauer properties of bismuth substituted nanosized cobalt ferrites through glycine nitrate synthesis method, Journal of Applied Physics, 122 (2017).

[10] L. Kumar, P. Kumar, A. Narayan, M. Kar, Rietveld analysis of XRD patterns of different sizes of nanocrystalline cobalt ferrite, International Nano Letters, 3 (2013) 1-12.

[11] V. Senthil, J. Gajendiran, S.G. Raj, T. Shanmugavel, G.R. Kumar, C.P. Reddy, Study of structural and magnetic properties of cobalt ferrite (CoFe2O4) nanostructures, Chemical Physics Letters, 695 (2018) 19-23.

[12] H.K. Dubey, C. Verma, U. Rai, A. Kumar, P. Lahiri, Synthesis, characterization and properties of nickel based zinc ferrite nanoparticles, DOI (2019).

[13] T. Tatarchuk, M. Myslin, I. Mironyuk, M. Bououdina, A.T. Pędziwiatr, R. Gargula, B.F. Bogacz, P. Kurzydło, Synthesis, morphology, crystallite size and adsorption properties of nanostructured Mg–Zn ferrites with enhanced porous structure, Journal of Alloys and Compounds, 819 (2020) 152945.

[14] S.R. Patade, D.D. Andhare, S.B. Somvanshi, P.B. Kharat, S.D. More, K.M. Jadhav, Preparation and characterisations of magnetic nanofluid of zinc ferrite for hyperthermia, Nanomaterials and Energy, DOI (2020) 1-6.

[15] V.D. Mote, Y. Purushotham, B. Dole, Williamson-Hall analysis in estimation of lattice strain in nanometer-sized ZnO particles, Journal of theoretical and applied physics, 6 (2012) 1-8.

[16] H. Kumar, J.P. Singh, R. Srivastava, P. Negi, H. Agrawal, K. Asokan, FTIR and electrical study of dysprosium doped cobalt ferrite nanoparticles, Journal of Nanoscience, 2014 (2014) 862415.